Local characterization of light trapping effects of metallic and dielectric nanoparticles in ultra-thin Cu(In,Ga)Se_2 solar cells via scanning near-field optical microscopy

Min Song[a,b,*], Guanchao Yin[a] , Paul Fumagalli[b], Martina Schmid[a,b]
[a] Nanooptische Konzepte für die PV, Helmholtz-Zentrum Berlin, Hahn-Meitner-Platz 1, 14109 Berlin, Germany
[b] Institut für Experimentalphysik, Freie Universität Berlin, Arnimallee 14, 14195 Berlin, Germany

ABSTRACT

Plasmonic and photonic nanoparticles have proven beneficial for solar cells in the aspect of light management. For improved exploitation of nanoparticles in solar cells, it is necessary to reveal the absorption enhancement mechanism from the nanoparticles. In this study, we investigated the nanoparticle-enhanced solar cells in near-field regime with optic and opto-electric scanning near-field optical microscopy (SNOM). The near-field distribution of regularly arranged silver and polystyrene nanoparticles produced by nanosphere lithography on Cu(In,Ga)Se_2 (CIGSe) solar cells is characterized using a custom-built SNOM, which gives insight into the optical mechanism of light trapping from nanoparticles to solar cells. On the other hand, the photocurrent of CIGSe solar cells with and without nanoparticles is studied with an opto-electric SNOM by recording the photocurrent during surface scanning, further revealing the opto-electrical influences of the nanoparticles. In addition, finite element method simulations have been performed and agree with the results from SNOM. We found the dielectric polystyrene spheres are able to enhance the absorption and benefit the generation of charge carriers in the solar cells.

Keywords: scanning near-field optical microscopy, near field, nanoparticles, ultra-thin solar cells, aperture probe SNOM, photocurrent

1. INTRODUCTION

Due to their unique thermal, optical, and electrical properties, metallic and dielectric nanoparticles have been studied and applied in various fields such as nano-sensors [1], drug carriers [2, 3], nanospectroscopy techniques [4, 5], waveguide structures [6,7] and photovoltaics [8]. In recent years, solar cells with thinner absorbers have attracted a lot of attention, due to their reduced consumption of rare material [9, 10]. However, the reduction of absorber layer thickness results in the incomplete absorption of incident light, which decreases the photocurrent density. In order to keep the current density, nanoparticles have been used for light trapping in thin-film solar cells [10, 11]. In order to tailor the nanoparticles for photovoltaics applications, the mechanisms of solar cell enhancement by integration of nanoparticles is worth to be studied not only in principal but also in experiment. In recent years, many studies have been reported about the interaction between nanoparticles and light in far-field measurement and near-field simulation. However, broad work on near-field investigation is still lacking. Additionally, few reports discuss about measurements of the photocurrent of solar cells with localized illumination.

Scanning near-field optical microscopy (SNOM) has been widely used in nano-optics due to its combination of high spatial and spectral resolution [12]. The interaction between nanoparticles and light can be investigated within sub-wavelength resolution by local illumination. The flexibility of the SNOM system guarantees the combination with various techniques and its application in different characterization such as biological [13], opto-electrics [14] and opto-magnetics [15] research. In this paper, we used SNOM not only for optics study but also for photocurrent measurement.

*e-mail: min.song@helmholtz-berlin.de; phone +49(0)30/8062-43721

Here we studied the nanoparticle-enhanced absorption of ultra-thin solar cells based on $Cu(In,Ga)Se_2$ (CIGSe). CIGSe solar cells contain the rare element indium (In) in the absorber. In order to minimize the consumption of In, the absorber layer has been reduced from the standard 2 μm to less than 500 nm for ultra-thin solar cells, which also reduces the absorption efficiency. Thus, regularly arranged silver and polystyrene (PS) particles were fabricated on the top of ultra-thin CIGSe solar cells to enhance the absorption. In order to understand the near-field mechanism of nanoparticle-enhanced solar cells in experiment, we investigated the optics and the generation of charge carriers by using illumination mode SNOM with a localized light source confined by an aperture fiber probe. During the contact mode scanning of the aperture probe across the sample surface, the reflection density or the photocurrent were recorded. Additionally, simulations with the finite-element method (FEM) of the optical response were performed to calculate the absorption and reflection. Comparing the experimental and simulation results, the nanoparticle-enhanced absorption in the CIGSe absorber layer was discussed.

2. METHODS

The nanoparticles on solar cells were fabricated by shadow nanosphere lithography and thermal processing. Near-field optics and localized photocurrent were measured using two custom-built SNOM setups. The preparation details of ultra-thin CIGSe solar cells can be found in Ref [16]. In this section, the experimental methods of shadow nanosphere lithography (SNSL) and SNOM as well as the FEM simulation model are specially discussed.

2.1 Shadow Nanosphere Lithography

The regularly arranged nanoparticles on top of the CIGSe solar cells were fabricated by SNSL [17]. A low-cost and easy-operation method was used for fabrication of close-packed PS sphere masks. The PS spheres used were 909 nm in diameter. 0.2 ml of purchased PS latex solution was mixed in a micro tube with 1 vol. % of styrene in ethanol in a volume ratio of 1:1. About 0.3 ml mixed solution was distributed slowly on the water surface in a clean glass Petri dish by using a curved glass pipette with 0.1-0.5 mm opening. After gently shaking the dish, a close-packed PS mask was formed on the water surface. The solar cells were submerged in the water carefully without touching the PS mask. By sucking out the water, the PS mask was transferred to the solar cells surface after overnight evaporation. The close-packed PS mask is shown in Fig. 1 (a). Due to the styrene, there is about 1-5% overlap between neighbouring PS spheres [17]. In order to vary the PS structures on our samples, the size and pitch distance of PS spheres were adjusted by plasma etching. After 10 min plasma etching, the close-packed PS mask turned into separated regularly arranged PS spheres with 700±15 nm diameters as shown in Fig. 1 (b).

In order to prepare regularly arranged silver particles, close-packed PS spheres were used as a mask during the deposition of 250 nm silver film. Silver triangular particles formed on the surface after washing away the PS mask by toluol in ultra-sonic bath as shown in Fig. 1 (c). After annealing at 300 °C for 20 min, spherical silver particles with 200±30 nm diameters formed as shown in Fig. 1 (d). The size of the silver particles can be adjusted by controlling the thickness of silver deposition or the size of PS spheres.

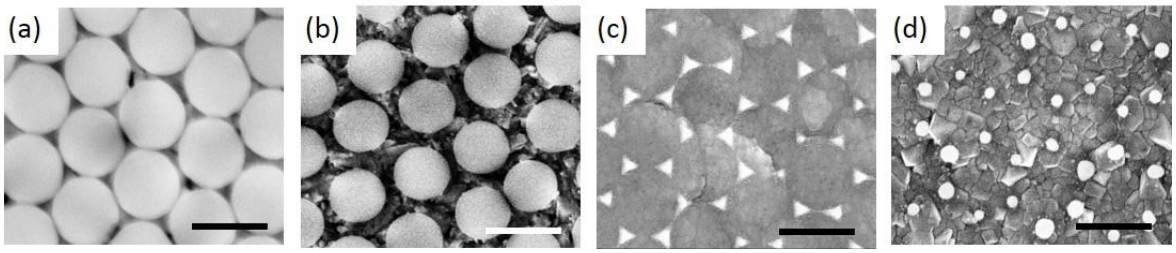

Fig. 1 SEM images of different nanoparticles on CIGSe solar cells. Scale bars represent 1 μm. (a) Close-packed PS spheres. The diameters are 909 nm. (b) PS spheres after plasma etching. (c) Regularly arranged silver triangles after silver deposition and removing the PS mask. (d) Regularly arranged silver spherical particles after annealing. The diameters are 200±30 nm.

2.2 Custom-built SNOM system

As the nanotechnology developed, many powerful tools have been created for the nanoparticle study. Among them, SNOM has been used in various research fields and applications, due to its high resolution, almost no limit for samples, non-request of vacuum working environment, flexibility of combination with different techniques, easy operation and low cost. As shown in Fig. 2 (a), SNOM is based on a sharp scanning probe on the sample surface, which can give a spatial resolution within the 100 nm regime. During the scanning, the interaction between the probe and the sample surface can be investigated with different detectors. A spectrometer or charge-coupled device (CCD) camera can be used to obtain the near-field optical signal as reflection or transmission or photoenergy spectrum [12]. By combining the SNOM with a photocurrent detector, one can analyze the generation of charge carriers due to the localized light illumination [14].

Here we investigated the optical interaction between nanoparticles and ultra-thin CIGSe solar cells by analyzing the reflection obtained via SNOM. By using the opto-electric SNOM, we studied the generation of charge carriers in the ultra-thin CIGSe solar cells under the localized illumination from an aperture probe. The basic setup is shown in Fig. 2 (a), the topography scanning unit is the same for both SNOMs: an aluminium-coated tapered fiber probe attached to a tuning fork was used as an aperture probe for topography characterization under contact scanning mode. A continuous wave laser at 532 nm was coupled into the aperture fiber probe and a localized field was generated at the end of the aperture, which was used as the illumination source as shown in Fig. 2 (b). However, the detection part was different. One of them is used for optics measurement with both illumination and collection modes [18]. Since the ultra-thin CIGSe solar cells have opaque molybdenum (Mo) back contact, only the reflection signal is recorded. During the scanning of the probe, the corresponding reflection signal was recorded by CCD camera and calculated to present the near-field distribution. The other detection part is connected to a photocurrent detector to analyze the generation of charge carriers in the contacted ultra-thin CIGSe solar cells. By recording the local photocurrent density while scanning the aperture probe across the sample surface, the correlation between photocurrent and topography was investigated.

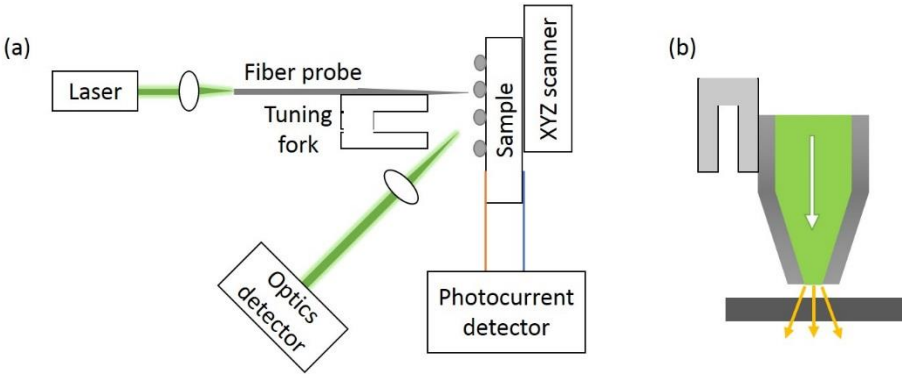

Fig. 2 (a) Sketch of SNOM system. We used different SNOM setups for optics and photocurrent detection. (b) Sketch of aperture fiber probe attached to tuning fork.

2.3 Finite element method

The finite element method (FEM) is a numerical technique for finding approximate solutions to boundary value problems for partial differential equations such as Maxwell's equations. It solves a large problem by calculating the situation in many individual small subparts which are called finite elements. The simple equations for each finite element are then combined with certain boundary conditions, resulting in the solution for the large domain.

Here we used the software package Comsol for FEM calculations of nanoparticles in solar cells. Since we studied regularly arranged particles on a relatively infinite surface, the simulation geometry was a hexagonal cylinder with periodic boundaries. Fig. 3 (a) represents the structure of the solar cells we studied. Figs. 3 (b) and (c) show the 3D simulation models of ultra-thin CIGSe solar cells with, respectively, PS nanoparticles and silver nanoparticles on top. The front-electrode material was aluminium (Al), and the back-electrode was thick Mo. The material properties and thickness values

of each layer as given in the figure were used for the simulation. Because the environment was infinite air, a perfectly matched layer (PML) boundary was added on the top of the model and its material was also defined as air. Additionally, since the back contact layer Mo was opaque and thick, another PML boundary was added at the bottom of the model and the material was defined as Mo. Light in the wavelength range of 350 - 1200 nm was incident perpendicularly to the surface of the solar cells. The incident port was set at the interface of air domain and PML domain. Absorption in each layer of the solar cells, absorption in the nanoparticles and total reflection at the incident port were calculated as a function of wavelength. By comparing the absorption of the $Cu(In,Ga)Se_2$ layer (Abs%_CIGSe) and the total reflection (R%) of the model with and without nanoparticles, the optical influence of the nanoparticles was evaluated.

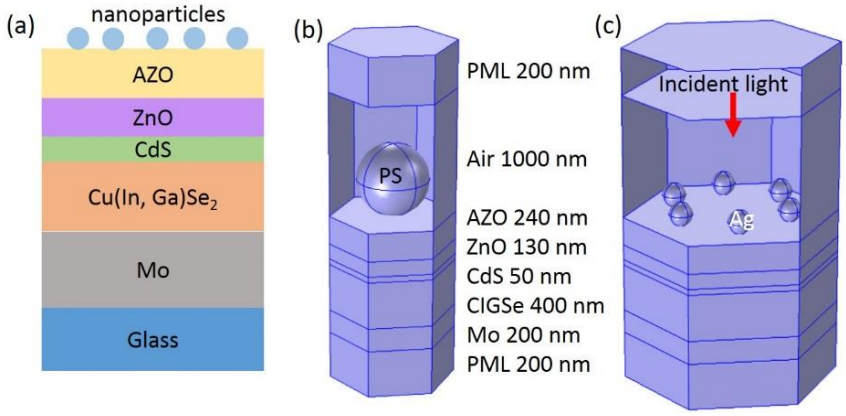

Fig. 3 (a) Structure of ultra-thin CIGSe solar cells with regularly arranged nanoparticles on top. (b) and (c) sketches of 3D simulation models for ultra-thin CIGSe solar cells with PS spheres and Ag particles, respectively. The multi-layers from top to bottom are top PML, air, Al:ZnO (AZO), ZnO, CdS, $Cu(In,Ga)Se_2$ (CIGSe), Mo and back PML.

3. RESULTS AND DISCUSSION

3.1 Regularly arranged silver particles

Silver particles can trap light by their unique plasmonic properties, which have been widely exploited in photovoltaics. Here we investigated the optical influence from regularly arranged silver particles fabricated with SNSL method on top of ultra-thin CIGSe solar cells.

Figs. 4 (a) and (b) show the near-field results. Comparing the reflection image in (b) with the corresponding topography in (a), a circular bright ring around the particle can be observed, which suggests there might be locally enhanced field. However, we did not find this enhancement in the photocurrent measurement. Figs. 4 (c) and (d) show the topography and photocurrent measurement results, respectively. The photocurrent distribution has no obvious correlation with the topography, but at the position of some nanoparticles the photocurrent was smaller.

In order to understand the influence of silver particles on solar cells, a corresponding simulation was performed. The simulation results shown in Fig. 4 (e) indicate that at short wavelength silver nanoparticles absorb light (green solid line) and increase the total reflection (red dashed line), resulting in a decrease of absorption in the CIGSe layer. In contrast, an anti-reflection effect from the silver particles and an enhancement of absorption in CIGSe were obtained at about 800 nm wavelength.

According to the simulation, two reasons for the decrease of absorption are expected. 200 nm silver nanoparticles have a parasitic absorption at 532 nm (wavelength for SNOM), and the backward scattering is significant from 350 nm to 750 nm [19]. Thus, the photocurrent of the solar cells is smaller under 532 nm light illumination after the incorporation of Ag nanoparticles.

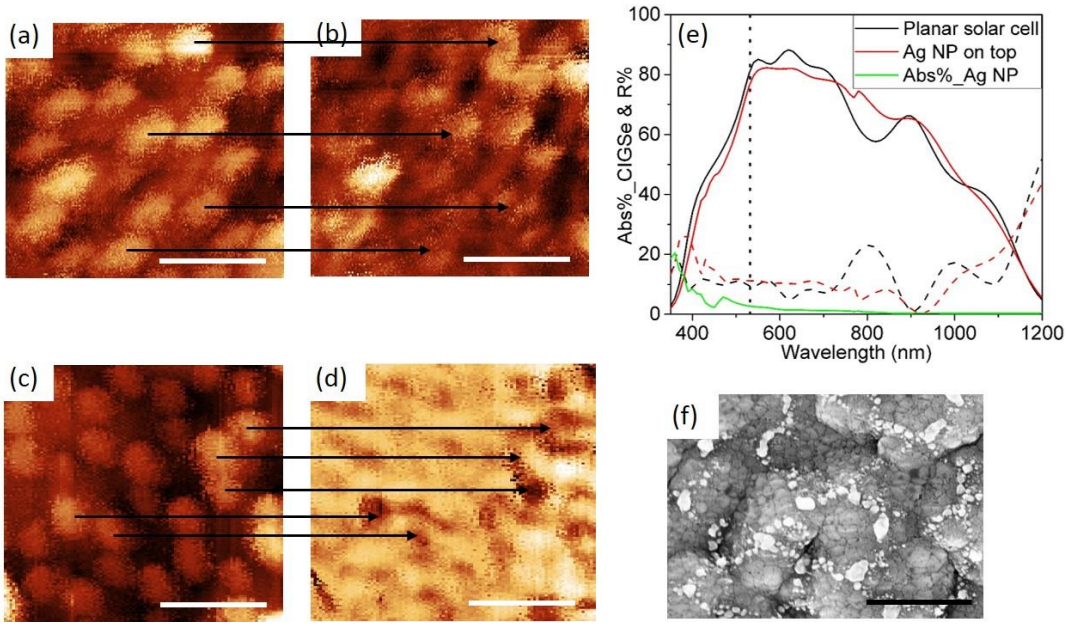

Fig. 4 (a) Topography of 200±30 nm regularly arranged silver particles on top of an ultra-thin CIGSe solar cell from SNOM with 532 nm light source. Scale bar represents 1 µm. (b) Corresponding near-field reflection result. (c) Topography of silver particles on top of solar cell from opto-electric SNOM with 532 nm light source. Scale bar represents 1 µm. (d) Corresponding photocurrent measurement. (e) Simulation of absorption in CIGSe absorber layer, silver nanoparticles and total reflection of solar cells with and without 200 nm regularly arranged silver nanoparticles on top. (f) SEM image of the Ag nanoparticle sample stored for three weeks. Scale bars represent 1 µm.

Another reason might be the diffusion of silver into the Al:ZnO top layer, since silver is a very active material [20]. This was proved by the SEM image of a sample after three weeks storage as shown in Fig. 4 (f). Some silver nanoparticle disappeared after three weeks and the boundaries of the remaining nanoparticles became blurred. The annealing step for silver nanoparticle fabrication may enhance the diffusion. The penetration of silver into the CIGSe solar cells will influence its properties or even damage the p-n junction.

3.2 Regularly arranged PS spheres

Comparing with the silver nanoparticles, dielectric nanoparticles have two advantages: no parasitic absorption and thermal stability. Dielectric nanostructures like SiO_2 particles have been studied in CIGSe solar cells and showed a good performance [10]. Here, we used the PS spheres with 909 nm diameter to fabricate close-packed monocrystalline structures on top of ultra-thin CIGSe solar cells. By controlling the plasma etching time, different structures can be prepared as represented in Figs. 5 (a) and (b). Fig. 5 (a) shows the sample etched for 15 min resulting in PS spheres around 580 nm in diameter. Fig. 5 (b) shows the sample etched for 30 min resulting in PS spheres around 300 nm in diameter. Center to center pitch remains 909 nm for both structures.

Corresponding simulations were performed with FEM and the results are shown in Fig. 5 (c). The solid lines present the absorption in the absorber layer (Abs%_CIGSe), and the dashed lines present the total reflection of the model (R%). The close-packed PS spheres (with 3% overlap between neighbouring spheres) increased the absorption in the CIGSe layer (red solid line) and decreased the total reflection (red dashed line) at the wavelength around 580 nm, 700 nm and 780 - 850 nm, which will result in the enhancement of the generation of charge carriers in solar cells. However, at the short wavelengths like 532 nm, the absorption decreased. As the diameters decreased from 909 nm to 580 nm, simulation gave an obvious absorption enhancement at the wavelengths around 500 - 600 nm and 740 - 850 nm (blue solid line). However, as the diameter decreased to 300 nm, the absorption in the CIGSe layer (green solid line) decreased and became even lower than for the planar solar cell (black solid line).

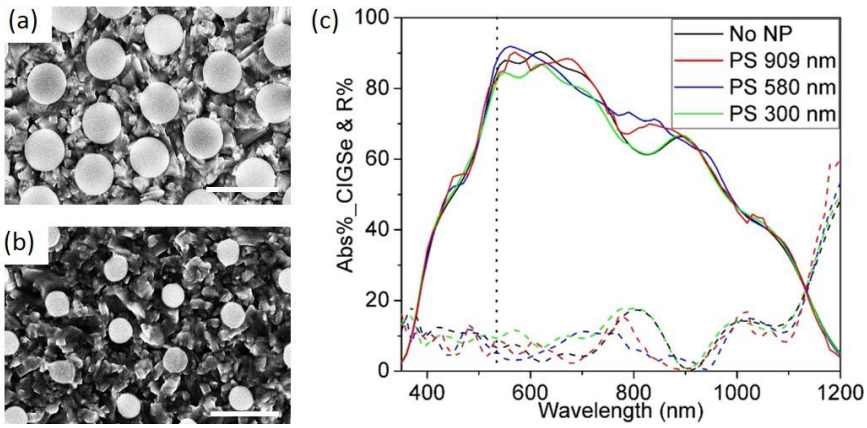

Fig. 5 (a) and (b) are SEM images of regularly arranged PS spheres on top of CIGSe solar cells fabricated with SNSL methods and plasma etching. Scale bars represent 1 μm. Spheres in (a) were etched for 15 min resulting in about 580 nm spheres, while spheres in (b) were etched for 30 min forming about 300 nm spheres. (c) Simulation prediction of absorption in absorber layer (solid lines) and total reflection (dashed lines) of CIGSe solar cells with different PS spheres on top.

According to the simulation results, we used our custom-built SNOM systems equipped with a 532 nm light source to measure the near-field optical properties and the photocurrent of CIGSe solar cells with 580 nm regularly arranged PS spheres on top. Fig. 6 (a) shows the topography of an area where a PS sphere was missing (black circle). The corresponding reflection signal was recorded as shown in Fig. 6 (b). Comparing with the area without PS spheres, the reflection is reduced in the area the PS spheres cover, indicating the PS spheres can direct more light into the solar cells. This can be correlated to the intrinsic scattering properties of dielectric nanoparticles, which preferentially scatter light in the forward direction [21, 22]. Additionally, a single PS sphere can behave as a near-field micro lens focusing the light into the solar cell [23].

The photocurrent measurement is shown in Fig. 6 (d) and Fig. 6 (c) is the corresponding topography image (not at the same position as Figs. 6 (a) and (b)). It is obvious that the photocurrent had an opposite distribution to that of reflection in Fig. 6 (b), which proves the anti-reflection and the focusing effect of PS spheres. Additionally, a slightly bright ring obtained in the photocurrent image is the signal from the gap between PS spheres which indicates the photocurrent of the planar solar cell. Comparing the local photocurrent density at the position of PS spheres and at the planar solar cell's surface, it is clear that the PS spheres gave a local enhancement of the photocurrent. A relatively darker ring was generated at the edge of the individual PS spheres, which proves the light focusing effect of the PS spheres.

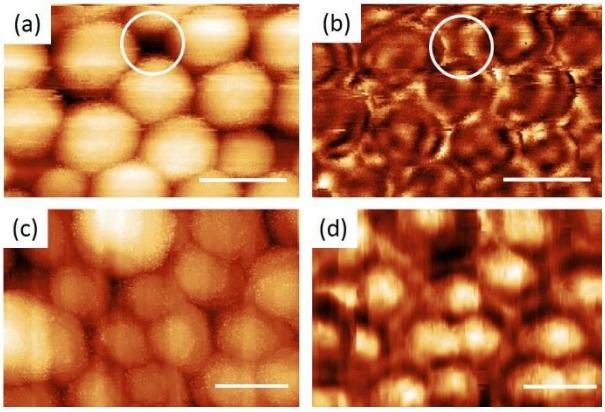

Fig. 6. Optical and opto-electrical SNOM measurements for 580 nm PS sphere on top of CIGSe solar cells. Scale bars represent 1 μm. (a) and (b) are, respectively, the corresponding topography and reflection images from optic SNOM measurement. (c) and (d) are corresponding topography and photon-current distribution images from opto-electric SNOM measurement.

4. CONCLUSION

In summary, by using two custom-built SNOM systems we have locally investigated the light trapping of regularly arranged silver particles and PS spheres on top of ultra-thin Cu(In,Ga)Se_2 solar cells and the generation of charge carriers. Regularly arranged silver particles were not found suitable to be added onto the solar cells due to their diffusion and absorption properties. On the other hand, PS spheres with certain diameters provided enhancement of absorption in the CIGSe layer and photocurrent generation. The main mechanism of this enhancement is the preferential scattering and focusing behaviour of dielectric PS spheres.

ACKNOWLEDGMENT

Regarding the SNOM setup, the collaboration with all members and technicians of the Fumagalli group from the Freie Universität Berlin is acknowledged. The authors are thankful to Michael Kirsch and Berit Heidmann for help with solar cell fabrication, as well as to Gauri Mangalgiri and Waseem Raja for discussions about simulation. Funding from the Helmholtz Association for the Young Investigator group VH-NG-928 within the Initiative and Networking fund is greatly acknowledged. Min Song specially acknowledges the support of funding from the China Scholarship Council.

REFERENCES

[1] Mayer, K. M., and Hafner, J. H., "Localized surface plasmon resonance sensors," Chemical Reviews, 111(6), 3828-3857 (2011).
[2] Lin, Q., Chen, J., Zhang, Z., and Zheng, G., "Lipid-based nanoparticles in the systemic delivery of siRNA," Nanomedicine, 9(1), 105-120 (2014).
[3] Pan, L., He, Q., Liu, J., Chen, Y., Ma, M., Zhang, L., and Shi, J., "Nuclear-targeted drug delivery of TAT peptide-conjugated monodisperse mesoporous silica nanoparticles," Journal of the American Chemical Society, 134(13), 5722-5725 (2012).
[4] Schuller, J. A., Barnard, E. S., Cai, W., Jun, Y. C., White, J. S., and Brongersma, M. L., "Plasmonics for extreme light concentration and manipulation," Nature Materials, 9(3), 193-204 (2010).
[5] Aksu, S., Yanik, A. A., Adato, R., Artar, A., Huang, M., and Altug, H., "High-throughput nanofabrication of infrared plasmonic nanoantenna arrays for vibrational nanospectroscopy," Nano Letters, 10(7), 2511-2518 (2010).
[6] Maier, A., Barclay, P. E., Johnson, T. J., Friedman, M. D., and Painter, O., "Low-loss fiber accessible plasmon waveguide for planar energy guiding and sensing," Applied Physics Letters, 84(20), 3990-3992 (2004).
[7] Février, M., Gogol, P., Aassime, A., Mégy, R., Delacour, C., Chelnokov, A., and Dagens, B., "Giant coupling effect between metal nanoparticle chain and optical waveguide," Nano Letters, 12(2), 1032-1037 (2012).
[8] Atwater, H. A., and Polman, A., "Plasmonics for improved photovoltaic devices," Nature Materials, 9(3), 205-213 (2010).
[9] Dahan, N., Jehl, Z., Hildebrandt, T., Greffet, J. J., Guillemoles, J. F., Lincot, D., and Naghavi, N., "Optical approaches to improve the photocurrent generation in Cu(In,Ga)Se_2 solar cells with absorber thicknesses down to 0.5 μm," Journal of Applied Physics, 112(9), 094902 (2012).
[10] Yin, G., Manley, P., and Schmid, M., "Light absorption enhancement for ultra-thin Cu ($In_{1-x}Ga_x$)Se_2 solar cells using closely packed 2-D SiO_2 nanosphere arrays," Solar Energy Materials and Solar Cells, 153, 124-130 (2016).
[11] Wang, E. C., Mokkapati, S., Soderstrom, T., Varlamov, S., and Catchpole, K. R., "Effect of nanoparticle size distribution on the performance of plasmonic thin-film solar cells: monodisperse versus multidisperse arrays," IEEE Journal of Photovoltaics, 3(1), 267-270 (2013).
[12] Hecht, B., Sick, B., Wild, U. P., Deckert, V., Zenobi, R., Martin, O. J., and Pohl, D. W., "Scanning near-field optical microscopy with aperture probes: Fundamentals and applications," The Journal of Chemical Physics,112(18), 7761-7774 (2000).
[13] Herrmann, M., Neuberth, N., Wissler, J., Pérez, J., Gradl, D., and Naber, A., "Near-field optical study of protein transport kinetics at a single nuclear pore," Nano letters, 9(9), 3330-3336 (2009).

[14] Tománek, P., Škarvada, P., Macků, R., and Grmela, L., "Detection and localization of defects in monocrystalline silicon solar cell," Advances in Optical Technologies, (2010).
[15] Silva, T. J., Schultz, S., and Weller, D., "Scanning near-field optical microscope for the imaging of magnetic domains in optically opaque materials," Applied Physics Letters, 65(6), 658-660 (1994).
[16] Yin, G., Brackmann, V., Hoffmann, V., and Schmid, M., "Enhanced performance of ultra-thin Cu(In,Ga)Se_2 solar cells deposited at low process temperature," Solar Energy Materials and Solar Cells, 132, 142-147 (2015).
[17] Kosiorek, A., Kandulski, W., Chudzinski, P., Kempa, K., and Giersig, M., "Shadow nanosphere lithography: simulation and experiment," Nano Letters, 4(7), 1359-1363 (2004).
[18] Andrae, P., Fumagalli, P., and Schmid, M., "Comparative scanning near-field optical microscopy studies of plasmonic nanoparticle concepts," In SPIE Photonics Europe, 91320-91320 (2014).
[19] Schmid, M., Manley, P., Ott, A., Song, M., and Yin, G., "Nanoparticles for light management in ultrathin chalcopyrite solar cells," Journal of Materials Research, 31(21), 3273-3289 (2016).
[20] Yin, G., Steigert, A., Andrae, P., Goebelt, M., Latzel, M., Manley, P., Lauermann, I., Christiansen, S., and Schmid, M., "Integration of plasmonic Ag nanoparticles as a back reflector in ultra-thin Cu(In,Ga)Se_2 solar cells," Applied Surface Science, 355, 800-804 (2015).
[21] Sun, W., Fu, Q., and Chen, Z., "Finite-difference time-domain solution of light scattering by dielectric particles with a perfectly matched layer absorbing boundary condition," Applied Optics, 38(15), 3141-3151 (1999).
[22] Fu, Y. H., Kuznetsov, A. I., Miroshnichenko, A. E., Yu, Y. F., and Luk'yanchuk, B., "Directional visible light scattering by silicon nanoparticles," Nature Communications, 4, 1527 (2013).
[23] Lee, J. Y., Hong, B. H., Kim, W. Y., Min, S. K., Kim, Y., Jouravlev, M. V., Bose, R., Kim, K. S., Hwang, I., Kaufman, L. J., Wong, C. W., Kim, P., and Wong, C. W., "Near-field focusing and magnification through self-assembled nanoscale spherical lenses," Nature, 460(7254), 498-501 (2009).